

## Inhibition of the Wnt Signaling Pathway by Idax, a Novel Dvl-Binding Protein

SHIN-ICHIRO HINO,<sup>1</sup> SHOSEI KISHIDA,<sup>1,2</sup> TATSUO MICHIEUE,<sup>3</sup> AKIMASA FUKUI,<sup>4</sup>  
IKUO SAKAMOTO,<sup>1</sup> SHINJI TAKADA,<sup>5,6</sup> MAKOTO ASASHIMA,<sup>3,4</sup>  
AND AKIRA KIKUCHI<sup>1\*</sup>

Department of Biochemistry, Hiroshima University School of Medicine, 1-2-3, Kasumi, Minami-ku, Hiroshima 734-8551,<sup>1</sup>  
PRESTO, Japan Science and Technology Corporation, Hiroshima,<sup>2</sup> Crest Project<sup>3</sup> and Department of Life Science  
(Biology),<sup>4</sup> University of Tokyo, Meguro-ku, Tokyo 153-8902, and Center for Molecular and Developmental Biology,  
Faculty of Science, Kyoto University, Kitashirakawa, Sakyo-ku, Kyoto 606-8502,<sup>5</sup> and Kondoh Differentiation  
Signaling Project, ERATO, Japan Science and Technology Corporation, Kyoto,<sup>6</sup> Japan

Received 5 June 2000/Returned for modification 6 July 2000/Accepted 12 October 2000

**In attempting to clarify the roles of Dvl in the Wnt signaling pathway, we identified a novel protein which binds to the PDZ domain of Dvl and named it Idax (for inhibition of the Dvl and Axin complex). Idax and Axin competed with each other for the binding to Dvl. Immunocytochemical analyses showed that Idax was localized to the same place as Dvl in cells and that expression of Axin inhibited the colocalization of Dvl and Idax. Further, Wnt-induced accumulation of  $\beta$ -catenin and activation of T-cell factor in mammalian cells were suppressed by expression of Idax. Expression of Idax in *Xenopus* embryos induced ventralization with a reduction in the expression of *siamois*, a Wnt-inducible gene. Idax inhibited Wnt- and Dvl- but not  $\beta$ -catenin-induced axis duplication. It is known that Dvl is a positive regulator in the Wnt signaling pathway and that the PDZ domain is important for this activity. Therefore, these results suggest that Idax functions as a negative regulator of the Wnt signaling pathway by directly binding to the PDZ domain of Dvl.**

Wnt proteins constitute a large family of cysteine-rich secreted ligands that control development in organisms ranging from nematode worms to mammals (69). In vertebrates, the Wnt signaling pathway regulates axis formation, organ development, and cellular proliferation, morphology, motility, and fate (7, 9, 18, 42). In the current model, the serine/threonine kinase glycogen synthase kinase 3 $\beta$  (GSK-3 $\beta$ ) targets cytoplasmic  $\beta$ -catenin for degradation in the Axin complex in the absence of Wnt (20, 75). As a result, cytoplasmic  $\beta$ -catenin levels are low. Axin has been shown to be important for the degradation of  $\beta$ -catenin (25). It forms a complex with GSK-3 $\beta$ ,  $\beta$ -catenin, and adenomatous polyposis coli protein (APC) (2, 13, 20, 22, 28, 52, 71) and promotes GSK-3 $\beta$ -dependent phosphorylation of  $\beta$ -catenin and APC (13, 19, 20, 71). Phosphorylated  $\beta$ -catenin forms a complex with Fbw1 (also known as  $\beta$ TrCP or FWD1), a member of the F-box protein family, resulting in the degradation of  $\beta$ -catenin by the ubiquitin and proteasome pathways (12, 29). Indeed, Axin inhibits Wnt-dependent  $\beta$ -catenin accumulation and T-cell factor (Tcf) activation (26, 52). Thus, Axin is a negative regulator of the Wnt signaling pathway. In addition, Axin is phosphorylated by GSK-3 $\beta$  and this phosphorylation stabilizes Axin, in contrast to that of  $\beta$ -catenin (70). When Wnt acts on its cell-surface receptor Frizzled, Dvl, a cytoplasmic protein, antagonizes the action of GSK-3 $\beta$ . The phosphorylation of  $\beta$ -catenin is reduced, it dissociates from the Axin complex, and  $\beta$ -catenin is no longer degraded, resulting in its accumulation in the cytoplasm. Accu-

mulated  $\beta$ -catenin is translocated into the nucleus where it binds to Tcf (also known as lymphocyte enhancer binding factor [Lef]), a transcription factor (3, 17, 43), and stimulates the expression of genes including *c-myc*, *fra*, *jun*, *cyclin D1*, and *peroxisome proliferator-activated receptor  $\delta$*  (PPAR $\delta$ ) (14, 15, 41, 55, 64).

Three Dvl genes, *Dvl-1*, *-2*, and *-3*, have been isolated in mammals (31, 48, 61). Expression of Dvl in cells induces the accumulation of  $\beta$ -catenin and the activation of Tcf (27, 35, 56). Dvl homologs are conserved in *Drosophila melanogaster* (Dishevelled [Dsh]) and *Xenopus laevis* (*Xenopus* dishevelled [Xdsh]) (30, 57, 65). Dsh mediates Wg signaling during embryogenesis and adult fly development, which in turn determines the ultimate cell fate in *Drosophila* (30, 65, 69). Genetic evidence shows that Dsh acts upstream of shaggy, a GSK-3 $\beta$  homolog, and antagonizes its functions. Expression of Dsh in the *Drosophila* imaginal disc cell line clone 8 causes the accumulation of Armadillo, a  $\beta$ -catenin homolog (72, 73). Expression of Xdsh induces a secondary body axis in *Xenopus* embryos, which is similar to the phenotype observed with expression of Wnt and  $\beta$ -catenin (44, 57). Thus, it is likely that Dvl and Dsh act as positive regulators of the Wnt signaling pathway. In addition to Wg signaling, Dsh mediates the planar tissue polarity signaling to determine cell polarity by activating Jun N-terminal kinase (JNK) through the small GTP-binding protein RhoA (4, 60). Dvl also plays a role in activating JNK in mammals (38, 45). Although the ligand that is responsible for *Drosophila* planar tissue polarity signaling has not been identified, Wnt-11 was shown to stimulate a vertebrate planar tissue polarity-like pathway (16, 62). Thus, Dvl and Dsh appear to regulate two distinct downstream pathways.

All Dsh and Dvl family members contain three highly conserved domains (7, 9, 42): an N-terminal DIX domain which is

\* Corresponding author. Mailing address: Department of Biochemistry, Hiroshima University School of Medicine, 1-2-3, Kasumi, Minami-ku, Hiroshima 734-8551, Japan. Phone: 81-82-257-5130. Fax: 81-82-257-5134. E-mail: akikuchi@mca.med.hiroshima-u.ac.jp.

also found in the C terminus of Axin; a central PDZ domain which has been shown to be a protein-protein interaction surface in several proteins; and a DEP domain which is conserved in proteins that regulate GTP-binding proteins. The high conservation of these three domains of Dsh and Dvl reflects their conserved properties. Indeed, several studies demonstrated the functional significance of the DIX and DEP domains. The DEP domain of Dsh has been found to be critical for rescue of the *Drosophila* Dsh planar polarity defect and for the activation of JNK but not essential for the Wg pathway (4, 60). The DEP domain of vertebrate Dvl is necessary for JNK activation in mammals but not for axis formation (38, 45). The DIX domain is important for axis formation and the Wg and Wnt signaling pathways (1, 45, 49). In contrast, the findings concerning the PDZ domain are variable. For example, it was shown previously that disruption of the PDZ domains of Dsh and Dvl abolishes their activity in the Wg and Wnt signaling pathways and in the *Xenopus* secondary axis formation, suggesting that the PDZ domain is essential for the Wnt signaling pathway (57, 73). However, it has been recently reported that the PDZ domain is dispensable for secondary axis formation in *Xenopus* embryos and that it may be important for maintaining the active conformation of Dvl (49). The inconsistency between these results could be due to a difference in the degree of deletion in the PDZ domain. Therefore, the roles of the PDZ domain of Dvl in the Wnt signaling pathway are not clear.

Dvl antagonizes the ability of Axin to induce ventralization in *Xenopus* embryos (76). Consistent with these results, Dvl interacts with Axin (10, 27, 56) and inhibits GSK-3 $\beta$ -dependent phosphorylation of  $\beta$ -catenin, APC, and Axin in the Axin complex (27, 70). In addition, it has been shown that Dvl forms a complex with the Axin-related protein (XARP) in *Xenopus* embryos and that the expression of Dvl induces the displacement of GSK-3 from its complex with XARP (21). Therefore, Dvl may also induce the dissociation of GSK-3 $\beta$  from Axin. The DIX and PDZ domains are important for the complex formation between Dvl and Axin (10, 27, 56). However, how the interaction of Dvl with Axin is regulated is not known. In our efforts to clarify further the roles of Dvl in the Wnt signaling pathway, we isolated a novel protein which binds to the PDZ domain of Dvl by the yeast two-hybrid screening. We designated this protein Idax (for inhibition of the Dvl and Axin complex). We show here that Idax inhibits the Wnt-dependent accumulation of  $\beta$ -catenin and activation of Tcf in mammalian cells. Moreover, we demonstrate that Idax suppresses Wnt- and Dvl-induced but not  $\beta$ -catenin-induced axis duplication in *Xenopus* embryos. These results suggest that Idax acts as a negative regulator of the Wnt signaling pathway by interacting with Dvl.

#### MATERIALS AND METHODS

**Materials and chemicals.** pTOPFLASH, pFOPFLASH, and pUC/EF-1 $\alpha$ / $\beta$ -catenin<sup>SA</sup> and XBC40 (X $\beta$ -catenin expression vector for *Xenopus* injection) were provided by H. Clevers (University Hospital, Utrecht, The Netherlands), A. Nagafuchi (Kyoto University, Kyoto, Japan), and D. Kimelman (University of Washington, Seattle, Wash.), respectively. The cDNA of human Dvl-1, and the anti-glutathione S-transferase (anti-GST) and the anti-maltose binding protein (anti-MBP) antibodies were provided by B. Dallapiccola (Vergata University, Rome, Italy) (48) and M. Nakata (Sumitomo Electronics, Yokohama, Japan), respectively. The MBP- and GST-fused proteins were purified from *Escherichia coli* according to the manufacturer's instructions. The anti-Axin and the anti-Dvl antibodies were prepared in rabbits by immunization with recombinant proteins of rAxin-(89-216) and Dvl-1-(1-140), respectively (50, 70). The anti-Myc anti-

body was prepared from 9E10 cells. L cells stably expressing Idax were generated by selecting with G418 as described previously (26). Wnt-3a conditioned medium was generated as already described (54). The anti- $\beta$ -catenin antibodies were purchased from Transduction Laboratories (Lexington, Ky.). [ $\alpha$ -<sup>32</sup>P]dCTP and Cy5-labeled anti-mouse immunoglobulin G (IgG) were obtained from Amersham Pharmacia Biotech Ltd. (Little Chalfont, Buckinghamshire, United Kingdom). The Alexa 546-labeled anti-rabbit IgG and the anti-green fluorescent protein (anti-GFP) antibody were purchased from Molecular Probes, Inc. (Eugene, Oreg.). Mouse embryo MTN blot was purchased from Clontech Laboratories, Inc. (Palo Alto, Calif.). Other materials were from commercial sources.

**Plasmid construction.** pBJ-Myc/rAxin, pMAL-c2/rAxin, pBJ-Myc/Dvl-1, pCGN/Dvl-1, and pGEX-2T/Dvl-1-(1-140) were constructed as described previously (20, 27, 28). Standard recombinant DNA techniques were used to construct the following plasmids: pEF-BOS-HA/Idax, pBSKS/Idax, pMAL-c2/Idax, pMAL-c2/Idax-(1-108), pMAL-c2/Idax-(109-198), pBTM16HA/Dvl-1-(251-336), pGEX-2T/Dvl-1-(251-336), pBSKS/Dvl-1-(337-670), pEF-BOS-Myc/Dvl-1-(224-371), pEF-BOS-Myc/Dvl-1-(337-670), pGEX-4T-1/Dvl-1-(395-670), pGEX-2T/Dvl-1-(1-250), pEF-BOS-Myc/Dvl-1-(1-378), pGEX-2T/Dvl-1-(1-378), pEGFP-C3/Dvl-1, pEF-BOS-HA/hTcf-4E, pBJ-Myc/hTcf-4E, pEF-BOS-Myc/GSK-3 $\beta$ , and pBJ-Myc/ $\beta$ -catenin. In these plasmids, some plasmid constructions were done by digesting the original plasmids with restriction enzymes and inserting the fragments into the vectors. Other constructions were done by inserting the fragments generated by the Expand high fidelity PCR system (Roche Diagnostics GmbH, Mannheim, Germany) into the vectors. The entire PCR products were sequenced, and the structures of all plasmids were confirmed by restriction analysis.

**Immunocytochemistry.** L cells grown on coverslips were fixed for 20 min in phosphate-buffered saline (PBS) containing 4% paraformaldehyde. The cells were washed with PBS three times and then were permeabilized with PBS containing 0.1% Triton X-100 and 2 mg of bovine serum albumin/ml for 20 min. The cells were washed and incubated for 1 h with the antihemagglutinin (anti-HA) or the anti-Axin antibody. After being washed with PBS, they were further incubated for 1 h with Cy5-labeled anti-mouse and Alexa 546-labeled anti-rabbit immunoglobulin G (IgG). The coverslips were washed with PBS, mounted on glass slides, and viewed with a confocal laser-scanning microscope (LSM510; Carl Zeiss).

**Interaction of Idax with Dvl.** To determine whether Idax interacts with Dvl in intact cells, L cells stably expressing HA-Idax (L-Idax cells) (6-cm-diameter dish) transfected with pBJ-Myc-derived plasmids were lysed in 200  $\mu$ l of lysis buffer (20 mM Tris-HCl [pH 7.5], 150 mM NaCl, 20  $\mu$ g of leupeptin/ml, 20  $\mu$ g of aprotinin/ml, 1 mM phenylmethylsulfonyl fluoride, 1% Nonidet P-40, and 10% glycerol) and the lysates were centrifuged at 15,000  $\times$  g for 10 min at 4°C. The supernatant (150  $\mu$ g of protein) was immunoprecipitated with the anti-Myc antibody, and then the precipitates were probed with the anti-Myc and anti-HA antibodies. To examine the interaction of Idax with Dvl-1 using purified proteins in vitro, 1  $\mu$ M GST-Dvl-1 mutants was incubated with MBP-Idax or its deletion mutants (30 pmol) immobilized on amylose resin in 100  $\mu$ l of low-salt buffer (20 mM Tris-HCl [pH 7.5] and 1 mM dithiothreitol) for 1 h at 4°C. MBP fusion proteins were precipitated by centrifugation, and the precipitates were washed successively with NP-40 buffer (20 mM Tris-HCl [pH 7.5], 150 mM NaCl, 1% Nonidet P-40, and 10% glycerol), LiCl buffer (0.1 M Tris-HCl [pH 7.5] and 0.5 M LiCl), and low-salt buffer, and then the precipitates were probed with the anti-GST antibody. To show inhibition by Idax of the binding between Axin and Dvl-1, the given concentrations of MBP-Idax and 1  $\mu$ M MBP-rAxin were incubated with GST-Dvl-1-(1-378) (5 pmol) immobilized on glutathione Sepharose 4B in 100  $\mu$ l of low-salt buffer containing 0.5% 3-[(3-cholamidopropyl)dimethylammonio] propanesulfonic acid. GST-Dvl-1-(1-378) was precipitated by centrifugation, and the precipitates were probed with the anti-MBP and anti-GST antibodies. In the reciprocal experiments the given concentrations of MBP-rAxin and 2  $\mu$ M MBP-Idax were incubated with GST-Dvl-1.

**Luciferase assay and  $\beta$ -catenin accumulation in L and 293 cells.** To examine the effects of Idax on Wnt-3a-induced accumulation of  $\beta$ -catenin in L cells, after L cells stably expressing Neo (control L cells [L/C cells]) or L-Idax cells (35-mm-diameter dish) were deprived of serum for 6 h, they were treated with the indicated amounts of Wnt-3a conditioned medium. The cells were lysed in 100  $\mu$ l of NP-40 buffer, and the lysates (20  $\mu$ g of protein) were probed with the anti- $\beta$ -catenin antibody. To measure Wnt-3a-dependent Tcf-4 activity, L/C cells or L-Idax cells (35-mm-diameter dish) were transfected with pTOPFLASH, which contains optimal Tcf-binding sites, or pFOPFLASH, which contains mutated Tcf-binding sites (0.5  $\mu$ g), pEF-BOS-HA/hTcf-4E (0.1  $\mu$ g), and pME18S/lacZ (0.5  $\mu$ g) (26, 32). At 46 h after transfection, the cells were deprived of serum for 6 h and then were treated with 40  $\mu$ l of Wnt-3a-conditioned medium for 6 h. The cells were lysed, and luciferase activity was measured using a PicaGene (Toyo B-NET Co., Ltd., Tokyo, Japan) and lumiphotometer TD4000 (Futaba Medical,

Tokyo, Japan). To standardize the transfection efficiency, pME18S/lacZ carrying the SR $\alpha$  promoter linked to the coding sequence of the  $\beta$ -galactosidase gene was used as an internal control. To observe Dvl- and  $\beta$ -catenin-dependent Tcf-4 activation, pCGN/Dvl-1 (0.2  $\mu$ g), pUC/EF-1 $\alpha$ / $\beta$ -catenin<sup>SA</sup> (50 ng), and the indicated amounts of pEF-BOS-HA/Idax were transfected into 293 cells (35-mm-diameter dish) with pTOPFLASH or pFOPFLASH (0.5  $\mu$ g), pEF-BOS-HA/hTcf-4E (0.1  $\mu$ g), and pME18S/lacZ (0.5  $\mu$ g). After 46 h, the cells were lysed and luciferase activity was measured as described.

**Xenopus injections and analysis of phenotypes.** Xwnt-8 and Xglobin expression plasmids were constructed as described previously (71). Myc-tagged Idax, its deletion mutants, and Dvl-1 were individually subcloned into the *Bg*III site of pSP64T (34). Sense mRNA was obtained by in vitro transcription of linearized templates using the SP6-mMESSAGE mMACHINE kit (Ambion, Austin, Tex.). Fertilized eggs were dejellied using 4.5% cysteine acid, and mRNAs were injected into dorsal or ventral blastomeres at the four-cell stage. After injection, embryos were cultured for 3 days (at stage 40 to 41). UV light irradiation was performed as described previously (53). The phenotypes of the injected embryos were evaluated by the Dorsal-Anterior Index (DAI) (24). For reverse transcription-PCR (RT-PCR), injected embryos were incubated at stage 10.5, and then total RNA was isolated. Oligo(dT)-primed cDNAs were synthesized using 5  $\mu$ g of total RNA from 10 embryos. PCR analyses (35 cycles) were performed with ExTaq DNA polymerase (TaKaRa Shuzo Co., Ltd., Ohtsu, Japan). Primers for PCR were as follows: *EF-1 $\alpha$*  (5'-CAG ATT GGT GCT GGA TAT GC-3' and 5'-ACT GCC TTG ATG ACT CCT AG-3') and *siamois* (5'-AAG ATA ACT GGC ATT CCT GAG C-3' and 5'-GGT AGG GCT GTG TAT TTG AAG G-3').

**Others.** Yeast two-hybrid screening was carried out as previously described (20, 71). To obtain a full-length cDNA of Idax, the clone isolated by the yeast two-hybrid method was labeled with random primers and [ $\alpha$ -<sup>32</sup>P]dCTP and used to screen a  $\lambda$ ZAP rat brain cDNA library. Northern blot analysis was performed as already described (40). Protein concentrations were determined with bovine serum albumin as a standard (5). Rat brain cytosol was prepared as described previously (46).

**Nucleotide sequence accession numbers.** The GenBank accession numbers for rat *Idax* cDNA and human *Idax* cDNA are AF272158 and AF272159, respectively.

## RESULTS

**Identification of Idax.** To identify novel proteins involved in the Wnt signaling pathway, we screened a rat brain cDNA library by the yeast two-hybrid method using the PDZ domain of Dvl-1 as bait. Several clones were found to confer both His<sup>+</sup> and LacZ<sup>+</sup> phenotypes, and a full-length cDNA of one clone was isolated. This clone spanned a distance of 1,314 bp and contained an uninterrupted open reading frame of 594 bp, encoding a predicted protein of 198 amino acids (Fig. 1A). The first ATG was preceded by stop codons in all three reading frames. The neighboring sequence of the first ATG was consistent with the translation initiation start proposed by Kozak (33). Using the rat cDNA of this Dvl-binding protein as a probe, we isolated the human cDNA. The predicted amino acid sequence from human cDNA was identical to that from rat cDNA. By searching several databases, we found mouse expressed sequence tag clones (AW742348, AW989078, and AW045537) as highly conserved homologs of this Dvl-interacting protein. However, we did not find similar sequences in expressed sequence tag clones from *Drosophila* or *Caenorhabditis elegans*. Since this Dvl-interacting protein is a novel protein, we designated it Idax (for inhibition of the Dvl and Axin complex). The mRNA of *Idax* was highly expressed in cerebrum, cerebellum, and heart and was slightly expressed in thymus and testis among rat tissues (Fig. 1B). *Idax* mRNA was detected during development (embryonic days 7, 11, 15, and 17) of mouse embryos, with the highest expression at embryonic day 11 (Fig. 1C). The constructs of rat *Idax* and human Dvl-1 used in this study are shown in Fig. 1D.

**Interaction of Idax with Dvl.** Since Idax was isolated as a protein binding to Dvl by the yeast two-hybrid screening, we examined whether Idax forms a complex with Dvl in intact cells. To this end, we prepared L cells stably expressing HA-Idax (L-Idax cells) (Fig. 2A, lane 5). When Myc-Dvl-1 was expressed in L-Idax cells and the lysates were immunoprecipitated with the anti-Myc antibody, HA-Idax was detected in the Myc-Dvl-1 immune complexes (Fig. 2A, lanes 6 and 13). To determine which region of Dvl is responsible for complex formation with Idax, Myc-Dvl-1-(1-378) or Myc-Dvl-1-(337-670) was expressed in L-Idax cells (Fig. 2A, lanes 7 and 8). HA-Idax was immunoprecipitated with Myc-Dvl-1-(1-378) but not with Myc-Dvl-1-(337-670) (Fig. 2A, lanes 14 and 15). Further, the region containing the PDZ domain [Myc-Dvl-1-(224-371)] was sufficient for complex formation between Dvl and Idax (Fig. 2B, lane 4). These results indicate that Idax forms a complex with Dvl in intact cells and that the PDZ domain of Dvl is important for their interaction. Next, we examined whether HA-Idax forms a complex with other Wnt signaling molecules in intact cells. HA-Idax was not immunoprecipitated with Myc-rAxin, Myc- $\beta$ -catenin, Myc-Tcf-4, or Myc-GSK-3 $\beta$  in L cells (Fig. 2C, lanes 7 to 11).

To examine whether the interaction of Idax and Dvl is direct, deletion mutants of GST-fused Dvl-1 (GST-Dvl-1) and of MBP-fused Idax (MBP-Idax) were purified from *E. coli* (Fig. 2E, lanes 1 to 6; Fig. 2F, lanes 1 to 4). MBP-Idax precipitated endogenous Dvl from rat brain cytosol (Fig. 2D). GST-PDZ and GST-Dvl-1-(1-378) were precipitated with MBP-Idax immobilized on amylose resin, but GST-Dvl-1-(1-140), GST-Dvl-1-(1-250), GST-Dvl-1-(395-670), and GST were not (Fig. 2E, lanes 7 to 12). These GST-Dvl-1 mutants were not precipitated with MBP (Fig. 2E, lanes 13 to 17). GST-PDZ was precipitated with MBP-Idax-(109-198) but not with MBP-Idax-(1-108) (Fig. 2F, lanes 5 to 11). These results indicate that the C-terminal region of Idax binds directly to the PDZ domain of Dvl-1. In addition, Idax also bound to Dvl-3 (data not shown). Since the PDZ domains of Dvl-1, -2, and -3 are highly conserved (86% identity), Idax is expected to bind to these Dvls.

**Competition of Idax and Axin for their binding to Dvl.** Previously it was shown that Dvl interacts directly with Axin (27). GST-Dvl-1-(1-378), including the DIX domain and the PDZ domain, bound to MBP-rAxin, but GST-Dvl-1-(1-250) and the PDZ domain did not, suggesting that both the DIX and PDZ domains of Dvl are necessary for its interaction with Axin (Fig. 3A). Therefore, we examined whether Idax inhibits the binding of Dvl to Axin. MBP-Idax, but not MBP, competed with MBP-rAxin for the binding to GST-Dvl-1-(1-378) in a dose-dependent manner (Fig. 3B, lanes 1 to 6). In the reciprocal experiment, MBP-rAxin inhibited the binding of MBP-Idax to GST-Dvl-1-(1-378) (Fig. 3B, lanes 7 to 12). About 5  $\mu$ M Idax reduced the binding of 1  $\mu$ M Axin to Dvl by 50%, while approximately 1  $\mu$ M Axin decreased the binding of 2  $\mu$ M Idax to Dvl by 50%. These results suggest that the interaction of Idax with the PDZ domain is sufficient for interfering with complex formation between Dvl and Axin and that the affinity of Dvl for Axin is higher than that of Dvl for Idax. We also examined whether Idax and Axin competed with each other for the binding to Dvl in intact cells. HA-Idax formed a complex with GFP-fused Dvl-1 (GFP-Dvl-1) in L-Idax cells (Fig. 3C, lanes 2 and 5). When Myc-rAxin was expressed in L-Idax cells,

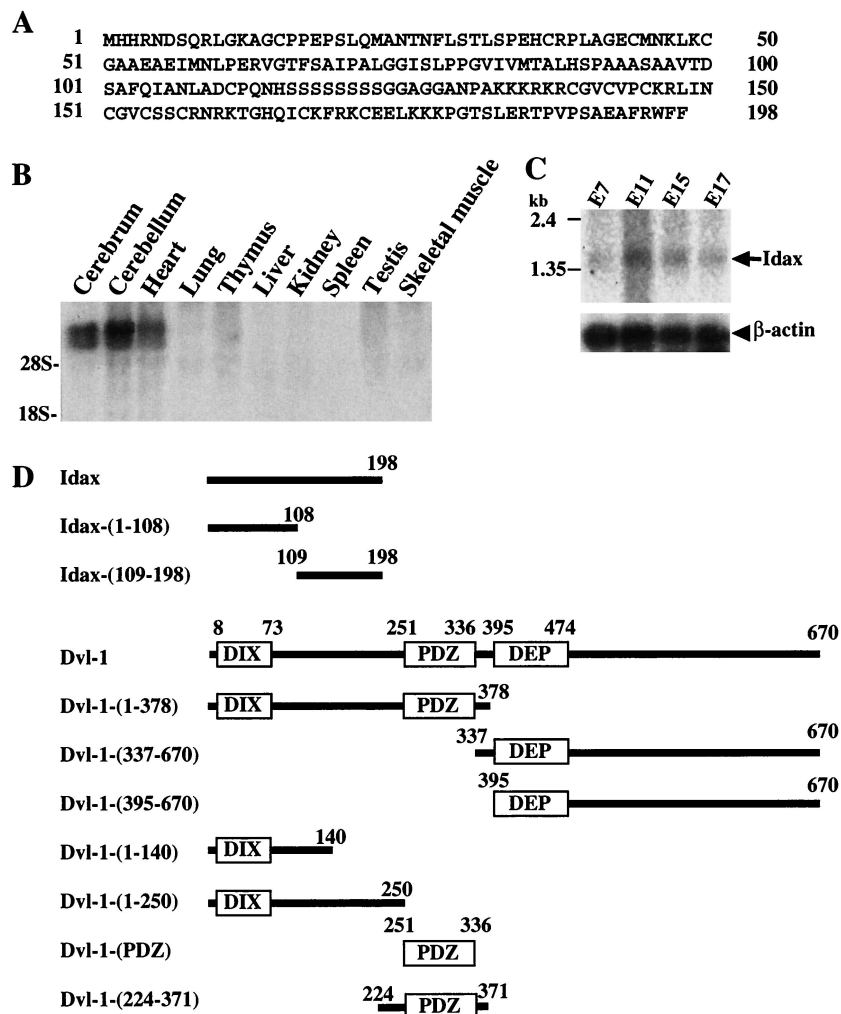


FIG. 1. Structure and gene expression of Idax. (A) Amino acid sequence of Idax. (B) Northern blot analysis of Idax in rat tissues. Total RNA (20  $\mu$ g per lane) from the indicated rat tissues was probed with full-length cDNA of rat Idax. The positions of 18S and 28S rRNA are indicated. (C) Northern blot analysis of Idax in mouse embryos. Poly(A) RNA (2  $\mu$ g per lane) from the indicated stages of mouse embryos was probed with the cDNAs of mouse  $\beta$ -actin and rat Idax-(369-495), which is identical with mouse Idax. E, embryonic day. (D) Schematic representation of deletion mutants of rat Idax and human Dvl-1 used in this study.

the association of HA-Idax with GFP-Dvl-1 was greatly reduced (Fig. 3C, lanes 3 and 6). These *in vitro* and intact cell studies suggest that Idax and Axin mutually inhibit their binding to Dvl.

**Subcellular localization of Idax.** We examined the localization of HA-Idax, GFP-Dvl-1, and Myc-rAxin in L cells using multiple immunofluorescence. HA-Idax showed a diffuse cytoplasmic pattern of expression with fine granules in L-Idax cells (Fig. 4A). Consistent with previous observations (10, 56), GFP-Dvl-1 was localized to distinct cytoplasmic vesicles in wild-type L cells (Fig. 4B and D). When GFP-Dvl-1 was expressed in L-Idax cells, the intracellular localization of HA-Idax was markedly changed. The localization of HA-Idax was similar to that of GFP-Dvl-1, and the merged image demonstrated that the two proteins colocalize (Fig. 4E, F, and G). Myc-rAxin had a diffuse cytoplasmic pattern of expression with some areas of particulate or vesicular staining in L cells (Fig. 4H). When Myc-rAxin was coexpressed with GFP-Dvl-1 in L cells, the two proteins were found to colocalize (Fig. 4I, J, and

K), consistent with previous observations (10, 56). These immunocytochemical studies demonstrate that Idax and Axin colocalize with Dvl. When GFP-Dvl-1 was coexpressed with Myc-rAxin in L-Idax cells, HA-Idax did not exhibit a vesicular pattern but showed a diffuse cytoplasmic pattern, although Myc-rAxin colocalized with GFP-Dvl-1 (Fig. 4L, M, N, and O).

**Effects of Idax on  $\beta$ -catenin signaling.** It was shown previously that Wnt-3a-conditioned medium induces the accumulation of  $\beta$ -catenin and activates Tcf-4 in L cells and that expression of Axin inhibits these Wnt-3a-dependent responses (26). Therefore, we examined the roles of Idax in Wnt signaling. Wnt-3a induced the accumulation of  $\beta$ -catenin in a dose-dependent manner in control L/C cells. Expression of Idax (L-Idax cells) suppressed this response (Fig. 5A). Similar results were obtained with three independent clones of L-Idax cells. Consistent with this result, Wnt-3a-dependent Tcf-4 activation was inhibited in L-Idax cells (Fig. 5B). Dvl-1 and  $\beta$ -catenin activated Tcf-4 in 293 cells (Fig. 5C, lanes 3 and 13), consistent with previous results (52, 56). Expression of Idax inhibited the

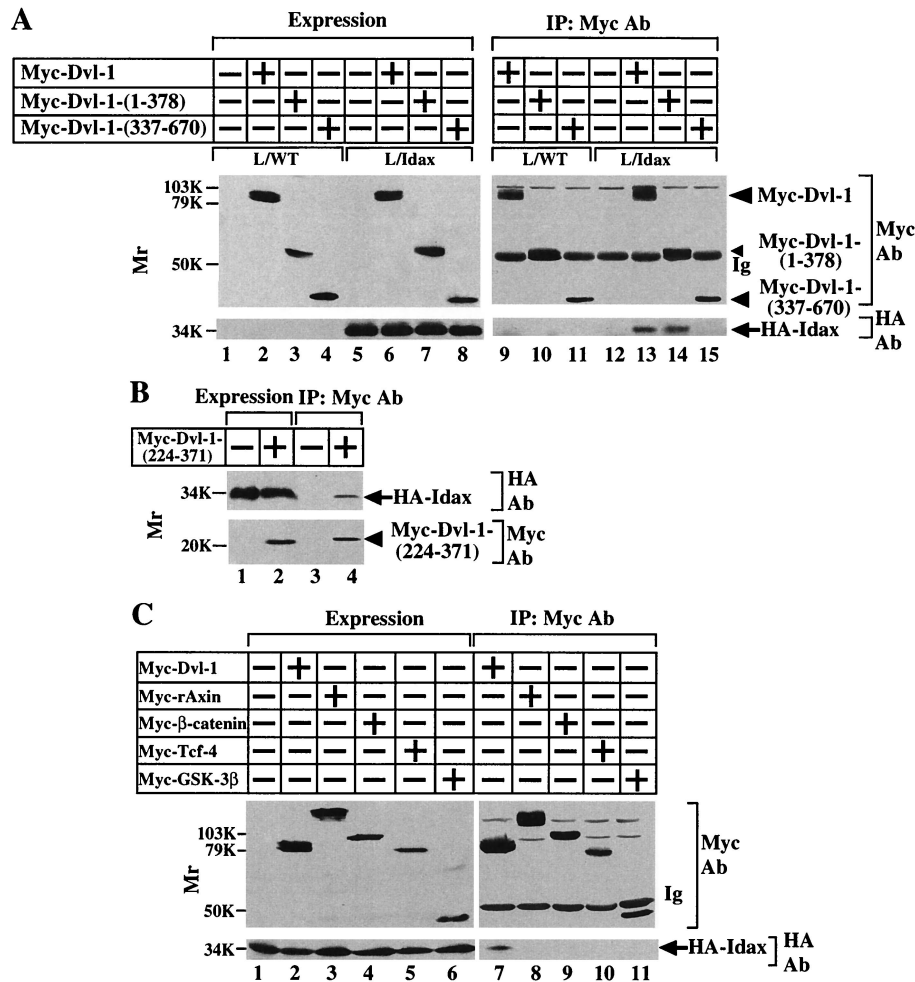


FIG. 2. Interaction of Idax with Dvl. (A) Interaction of Idax with Dvl in intact cells. The lysates (20  $\mu$ g of protein) of wild-type L cells (lanes 1 to 4) or L-Idax cells (lanes 5 to 8) expressing Myc-Dvl-1 (lanes 2 and 6), Myc-Dvl-1-(1-378) (lanes 3 and 7), or Myc-Dvl-1-(337-670) (lanes 4 and 8) were probed with the anti-Myc and anti-HA antibodies. The same lysates (150  $\mu$ g of protein) prepared in lanes 2 to 8 were immunoprecipitated with the anti-Myc antibody, and the immunoprecipitates were probed with the anti-Myc and anti-HA antibodies (lanes 9 to 15). IP, immunoprecipitation; Ab, antibody. (B) Interaction of Idax with the PDZ domain of Dvl. The lysates of L-Idax cells with (lane 2) or without (lane 1) expression of Myc-Dvl-1-(224-371) were probed with the anti-Myc and anti-HA antibodies. The same lysates (150  $\mu$ g of protein) prepared in lanes 1 and 2 were immunoprecipitated with the anti-Myc antibody, and the immunoprecipitates were probed with the anti-Myc and anti-HA antibodies (lanes 3 and 4). (C) Inability of Idax to bind to other Wnt signaling molecules. The lysates (20  $\mu$ g of protein) of L-Idax cells expressing Myc-Dvl-1 (lane 2), Myc-rAxin (lane 3), Myc- $\beta$ -catenin (lane 4), Myc-Tcf-4 (lane 5), or Myc-GSK-3 $\beta$  (lane 6) were probed with the anti-Myc and anti-HA antibodies. The same lysates (150  $\mu$ g of protein) prepared in lanes 2 to 6 were immunoprecipitated with the anti-Myc antibody, and the immunoprecipitates were probed with the anti-Myc and anti-HA antibodies (lanes 7 to 11). (D) Complex formation of Idax with Dvl in rat brain. Rat brain cytosol (30  $\mu$ g of protein) was probed with the anti-Dvl antibody (lane 1). The cytosol (100  $\mu$ g of protein) was incubated with MBP-Idax (lane 2) or MBP (lane 3) (30 pmol) immobilized to amylose resin, and MBP fusion proteins were precipitated by centrifugation and the precipitates were probed with the anti-Dvl antibody. (E) Direct interaction of Idax with Dvl. GST-Dvl-1-(1-140), GST-Dvl-1-(1-250), GST-Dvl-1-(1-378), GST-Dvl-1-PDZ, GST-Dvl-1-(395-670), and GST (1  $\mu$ g of protein) were stained with Coomassie brilliant blue (lanes 1 to 6). GST-Dvl-1-(1-140) (lanes 7 and 13), GST-Dvl-1-(1-250) (lanes 8 and 14), GST-Dvl-1-(1-378) (lanes 9 and 15), GST-Dvl-1-PDZ (lanes 10 and 16), GST-Dvl-1-(395-670) (lanes 11 and 17), or GST (lane 12) (1  $\mu$ M) was incubated with MBP-Idax (lanes 7 to 12) or MBP (lanes 13 to 17) (30 pmol) immobilized on amylose resin, and MBP fusion proteins were precipitated by centrifugation and the precipitates were probed with the anti-GST antibody. (F) The region of Idax which binds to Dvl. MBP-Idax, MBP-Idax-(1-108), MBP-Idax-(109-198), and MBP (0.5  $\mu$ g of protein) were stained with Coomassie brilliant blue (lanes 1 to 4). GST-Dvl-1-PDZ (lanes 5 to 8) or GST (lanes 9 to 11) (1  $\mu$ M) was incubated with MBP-Idax (lanes 5 and 9), MBP-Idax-(1-108) (lanes 6 and 10), MBP-Idax-(109-198) (lanes 7 and 11), or MBP (lanes 8) (30 pmol) immobilized on amylose resin. MBP fusion proteins were precipitated by centrifugation, and the precipitates were probed with the anti-GST antibody. The results shown are representative of three independent experiments.

Dvl-1-dependent but not the  $\beta$ -catenin<sup>SA</sup>-dependent activation of Tcf-4 (Fig. 5C).  $\beta$ -catenin<sup>SA</sup> is a  $\beta$ -catenin mutant which is not degraded due to the substitution of serine and threonine residues with alanine in the phosphorylation sites by GSK-3 $\beta$  (75). These results suggest that Idax acts as a negative regula-

tor of the Wnt signaling pathway and that it functions between Dvl and  $\beta$ -catenin.

**Regulation of axis formation by Idax.** To determine the mode of action of Idax, we examined the effects of Idax on the Wnt signaling pathway using *Xenopus* embryos. The Wnt sig-

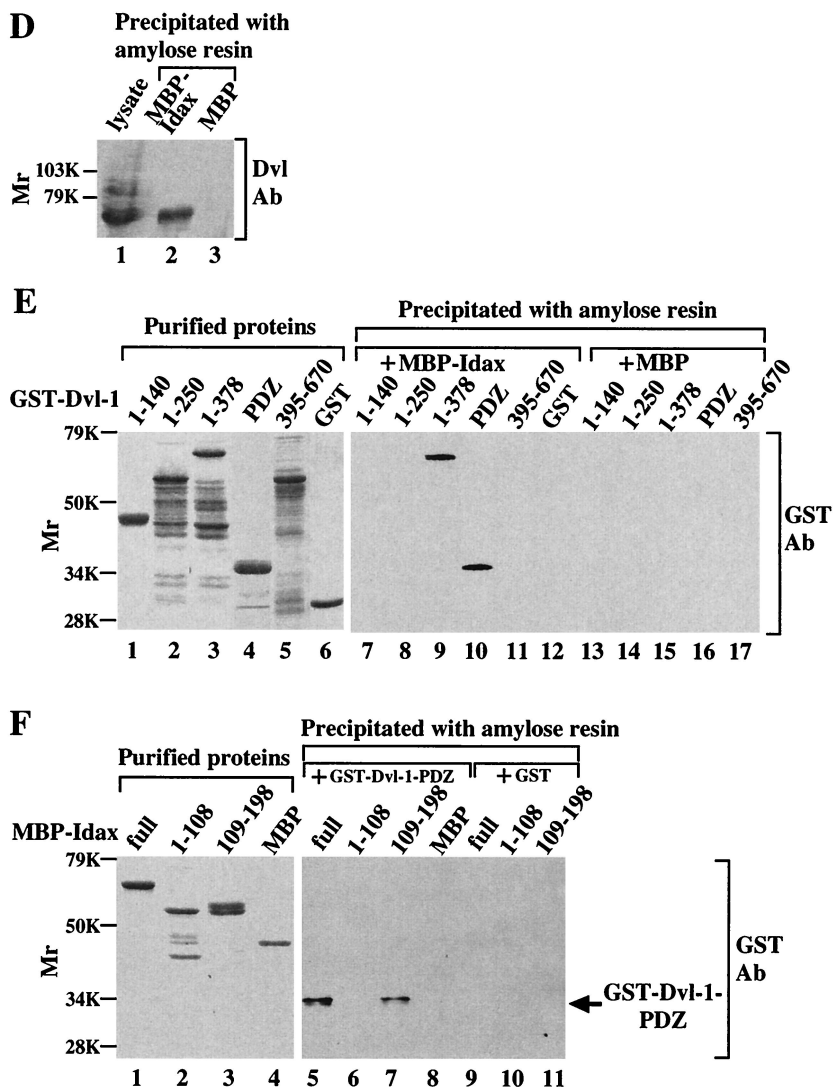


FIG. 2—Continued.

naling pathway regulates axis formation in *Xenopus* embryos (44). Dorsal and ventral injection of *Xglobin* mRNA into four-cell-stage embryos did not affect normal axis formation (Fig. 6A, a and b). Dorsal injection of *Idax* mRNA into embryos resulted in ventralization phenotypes such as loss of the head structure (Fig. 6A, c). Embryos injected ventrally with *Idax* mRNA developed normally (Fig. 6A, d). *siamois* is a homeobox gene which mediates the effects of the Wnt signaling pathway on axis formation and whose expression is activated by  $\beta$ -catenin-Tcf (6, 36). Expression of *siamois* was suppressed by dorsal but not ventral injection of *Idax* mRNA (Fig. 6B). When the mRNA of *Idax*(109-198) was injected dorsally, the embryos showed ventralizing phenotypes (Fig. 6C), while injection of the mRNA of *Idax*(1-108) had no effect (Fig. 6C). Therefore, *Idax* has ventralizing activity and the C-terminal region may be sufficient to regulate the embryonic axis formation, consistent with the observation that the C-terminal region of *Idax* has the Dvl-binding site.

Ventral injection of mRNAs of *Xwnt-8*, *Dvl*, or *X $\beta$ -catenin* has been shown to induce a secondary dorsal axis (11, 44, 57,

66) (Fig. 7A, a, c, and e). Coinjection of *Xwnt-8* and *Idax* in the ventral side repressed secondary axis formation (Fig. 7A, b). Similar phenotypes were observed upon coexpression of *Dvl-1* and *Idax* (Fig. 7A, d). In contrast, coinjection of *X $\beta$ -catenin* and *Idax* still induced the secondary axis structure (Fig. 7A, f). The effects of *Idax* on secondary axis formation by *Xwnt-8*, *Dvl*, or *X $\beta$ -catenin* are summarized in Fig. 7B. It was shown that UV light-irradiated embryos exhibit axial deficiencies (Fig. 7C, a) (53). *Idax* alone did not affect this phenotype (Fig. 7C, b). Consistent with previous observations, *Xwnt-8* rescued the UV-induced axial deficiencies (Fig. 7C, c). Coinjection with *Idax* inhibited this activity of *Xwnt-8* (Fig. 7C, d). *X $\beta$ -catenin* also rescued the UV-induced axial deficiencies (Fig. 7C, e), and coinjection with *Idax* did not affect *X $\beta$ -catenin*-dependent rescue of axis formation (Fig. 7C, f). The average DAI of the embryos is shown in Fig. 7D. Taken together, these results suggest that *Idax* negatively regulates the Wnt signaling pathway during *Xenopus* development downstream of Wnt and *Dvl* and upstream of  $\beta$ -catenin, consistent with the results observed in mammalian cells.

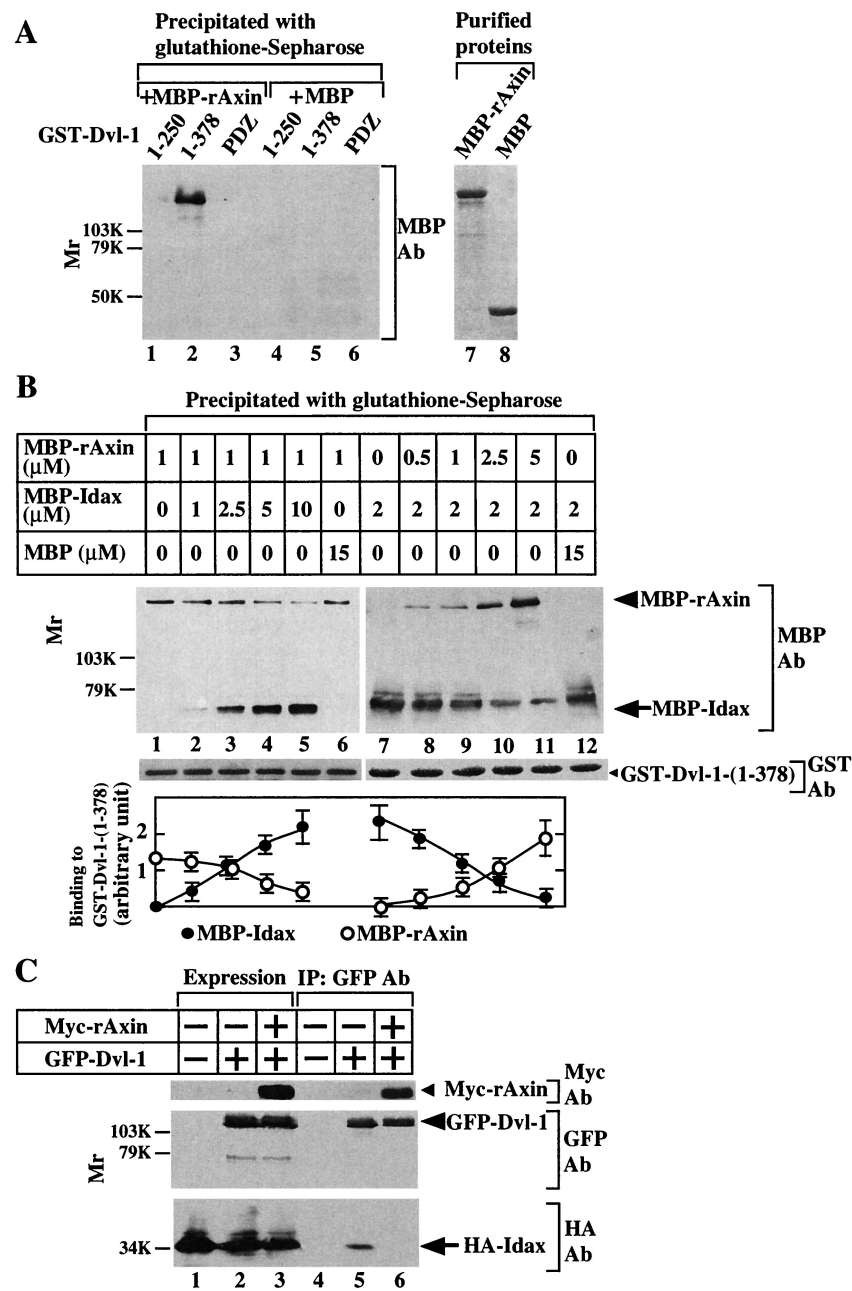


FIG. 3. Competition of Idax and Axin for their binding to Dvl. (A) Requirement of the DIX and PDZ domains of Dvl for its binding to Axin. After GST-Dvl-1-(1-250) (lanes 1 and 4), GST-Dvl-1-(1-378) (lanes 2 and 5), or GST-Dvl-1-PDZ (lanes 3 and 6) ( $0.5 \mu\text{M}$ ) was incubated with MBP-rAxin (lanes 1 to 3) or MBP (lanes 4 to 6) ( $0.5 \mu\text{M}$ ), the GST fusion proteins were precipitated by centrifugation and the precipitates were probed with the anti-MBP antibody. MBP-rAxin (lane 7) and MBP (lane 8) ( $0.5 \mu\text{g}$ ) were stained with Coomassie brilliant blue. (B) Competition of Idax and Axin for their binding to Dvl in vitro. MBP-rAxin ( $1 \mu\text{M}$ ) was incubated with GST-Dvl-1-(1-378) ( $5 \text{ pmol}$ ) immobilized on glutathione Sepharose 4B in the presence of the indicated concentrations of MBP-Idax (lanes 1 to 5) or MBP (lane 6). GST-Dvl-1-(1-378) was precipitated by centrifugation, and the precipitates were probed with the anti-MBP antibody (upper panel). The amounts of GST-Dvl-1-(1-378) precipitated in each binding assay are shown (middle panel). In reciprocal experiments, MBP-Idax ( $2 \mu\text{M}$ ) was incubated with GST-Dvl-1-(1-378) ( $5 \text{ pmol}$ ) immobilized on glutathione Sepharose 4B in the presence of the indicated concentrations of MBP-rAxin (lanes 7 to 11) or MBP (lane 12). The results shown in the upper and middle panels are representative of three independent experiments. The amounts of MBP-rAxin and MBP-Idax were analyzed using the NIH Image system and expressed as arbitrary units. The results shown are the mean  $\pm$  the standard error of three independent experiments (lower panel). (C) Inhibition of the binding of Idax to Dvl by Axin in intact cells. The lysates ( $20 \mu\text{g}$  of protein) of L-Idax cells transfected with empty vector (lane 1), pEGFPC1-Dvl-1 (lane 2), or pEGFPC1-Dvl-1 and pBJ-Myc/rAxin (lane 3) were probed with the anti-Myc, anti-GFP, and anti-HA antibodies. The same lysates ( $150 \mu\text{g}$  of protein) were immunoprecipitated with the anti-GFP antibody, and the immunoprecipitates were probed with the anti-Myc, anti-GFP, and anti-HA antibodies (lanes 4 to 6). IP, immunoprecipitation; Ab, antibody. The results shown are representative of three independent experiments.

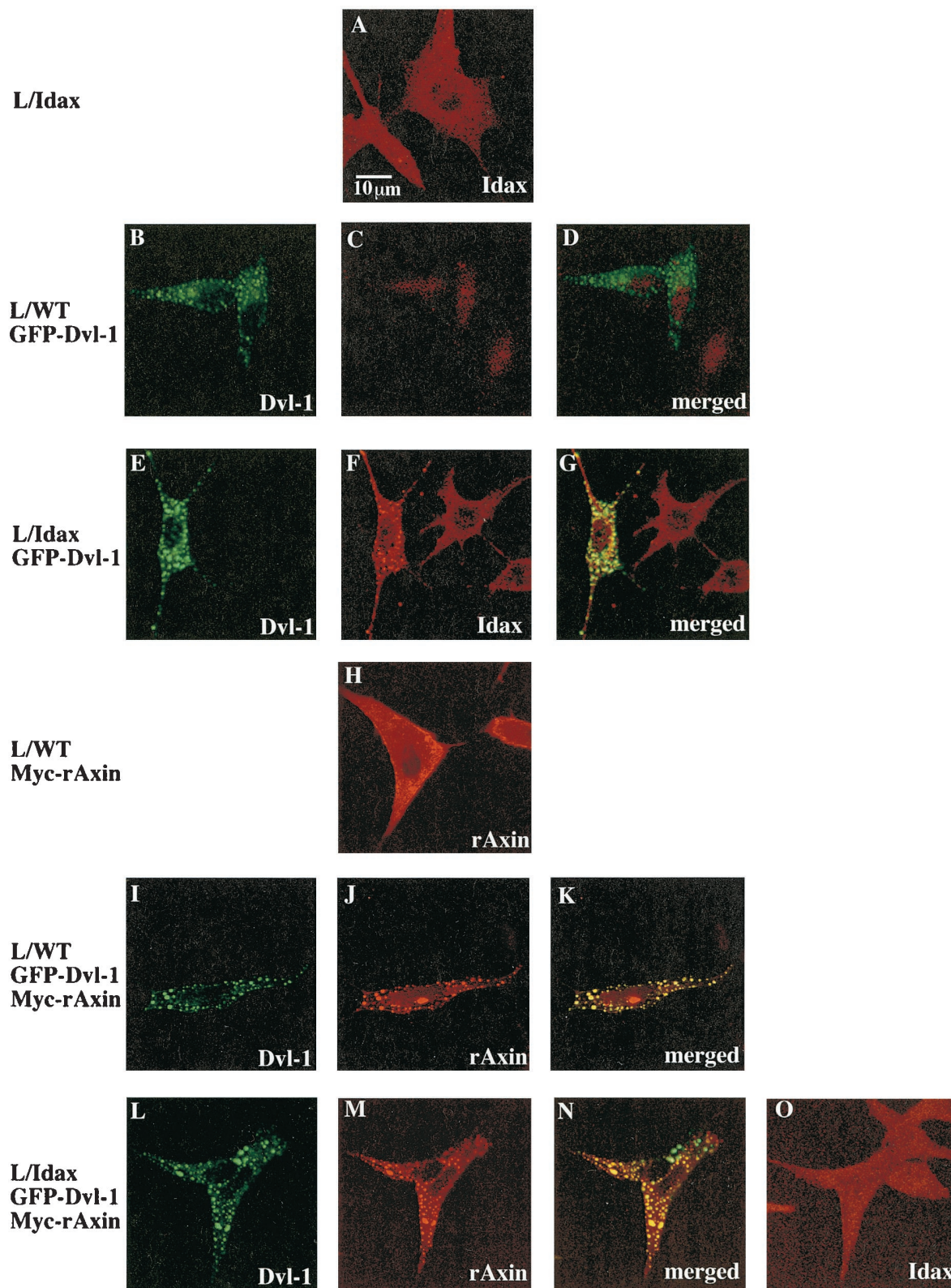


FIG. 4. Subcellular localization of Idax, Dvl-1, and rAxin. L-Idax cells (A), wild-type L cells expressing GFP-Dvl-1 (B, C, and D), L-Idax cells expressing GFP-Dvl-1 (E, F, and G), wild-type L cells expressing Myc-rAxin (H), wild-type L cells coexpressing GFP-Dvl-1 and Myc-rAxin (I, J, and K), and L-Idax cells coexpressing GFP-Dvl-1 and Myc-rAxin (L, M, N, and O) were fixed and permeabilized. Some of them were directly viewed with a confocal laser-scanning microscope to detect GFP-Dvl-1 (B, E, I, and L), and the others were stained with the anti-HA antibody to detect HA-Idax (A, C, F, and O) or with the anti-Axin antibody to observe Myc-rAxin (H, J, and M). Note that nuclei were stained nonspecifically with the anti-HA antibody. Merged pictures of panels B and C, E and F, I and J, and L and M are shown in panels D, G, K, and N, respectively. GFP-Dvl-1, Cy5-labeled HA-Idax, and Alexa 546-labeled Myc-rAxin produced no cross staining. The results shown are representative of three independent experiments.

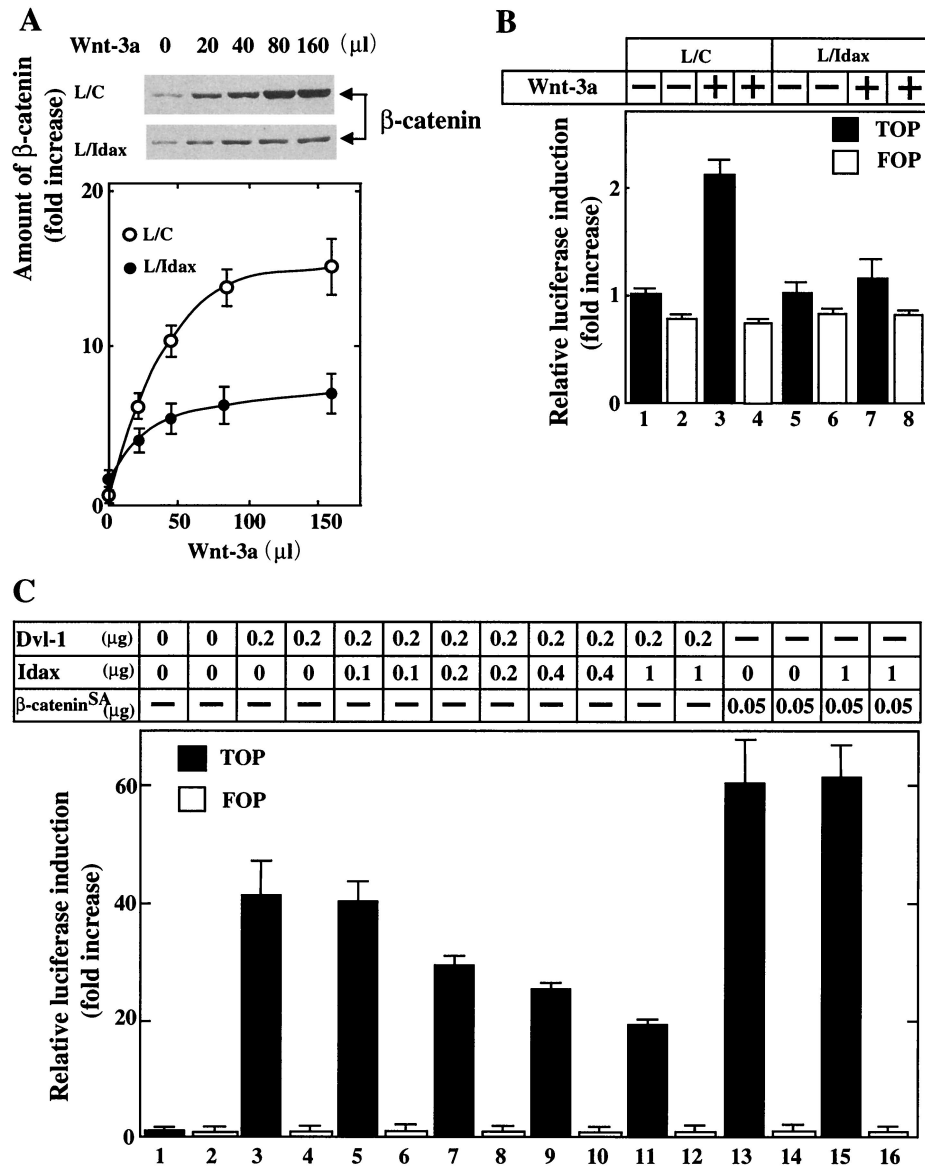


FIG. 5. Effects of Idax on  $\beta$ -catenin signaling. (A) Inhibition of Wnt-3a-induced accumulation of  $\beta$ -catenin by Idax. After L cells stably expressing Neo (control L cells [L/C]) (upper panel) and L-Idax cells (middle panel) were treated with the indicated amounts of Wnt-3a conditioned medium for 40 min, the cells were lysed and probed with the anti- $\beta$ -catenin antibody. The results shown in the upper and middle panels are representative of three independent experiments. The amounts of  $\beta$ -catenin were analyzed using the NIH Image system and expressed as fold increase compared with the level observed in L/C cells treated with control medium. The results shown are the mean  $\pm$  the standard error (SE) of three independent experiments (lower panel).  $\circ$ , L/C cells;  $\bullet$ , L-Idax cells. (B) Inhibition of Wnt-3a-induced Tcf activation by Idax. L/C cells (lanes 1 to 4) and L-Idax cells (lanes 5 to 8) transfected with pTOPFLASH (black bars) or pFOPFLASH (white bars) were treated with Wnt-3a-conditioned medium (lanes 3, 4, 7, and 8) or control medium (lanes 1, 2, 5, and 6) for 6 h. Luciferase activity was assayed and expressed as fold increase compared with the level observed in cells transfected with pTOPFLASH and treated with control medium. These results represent the mean  $\pm$  SE of five independent experiments. (C) Inhibition of Dvl- and  $\beta$ -catenin-dependent Tcf activation by Idax. pCGN-Dvl-1 and pEF-BOS-HA/Idax (lanes 3 to 12) or pUC/EF-1 $\alpha$ / $\beta$ -catenin<sup>SA</sup> and pEF-BOS-HA/Idax (lanes 13 to 16) were transfected into 293 cells with pTOPFLASH (black bars) or pFOPFLASH (white bars). After 46 h, luciferase activity was assayed and expressed as fold increase compared with the level observed in cells transfected with pTOPFLASH. These results represent the mean  $\pm$  SE of four independent experiments.

## DISCUSSION

In this study, we have isolated a novel protein which binds to the PDZ domain of Dvl directly and named it Idax. Idax suppresses the Wnt-3a-dependent accumulation of  $\beta$ -catenin and activation of Tcf in L cells. We have also shown that Idax inhibits axis formation and *siamois* expression in *Xenopus* embryos. Moreover, Idax suppresses Xwnt-8- and Dvl-induced

but not  $\beta$ -catenin-induced axis duplication and prevents Xwnt-8-dependent but not  $\beta$ -catenin-dependent rescue of the UV-irradiated ventralization. These results suggest that Idax acts between Dvl and  $\beta$ -catenin as a negative regulator of Wnt signaling. The Wnt signaling pathway plays essential roles in a number of developmental aspects, including gastrulation and organogenesis. For instance, Wnt-3 is required for mesoderm

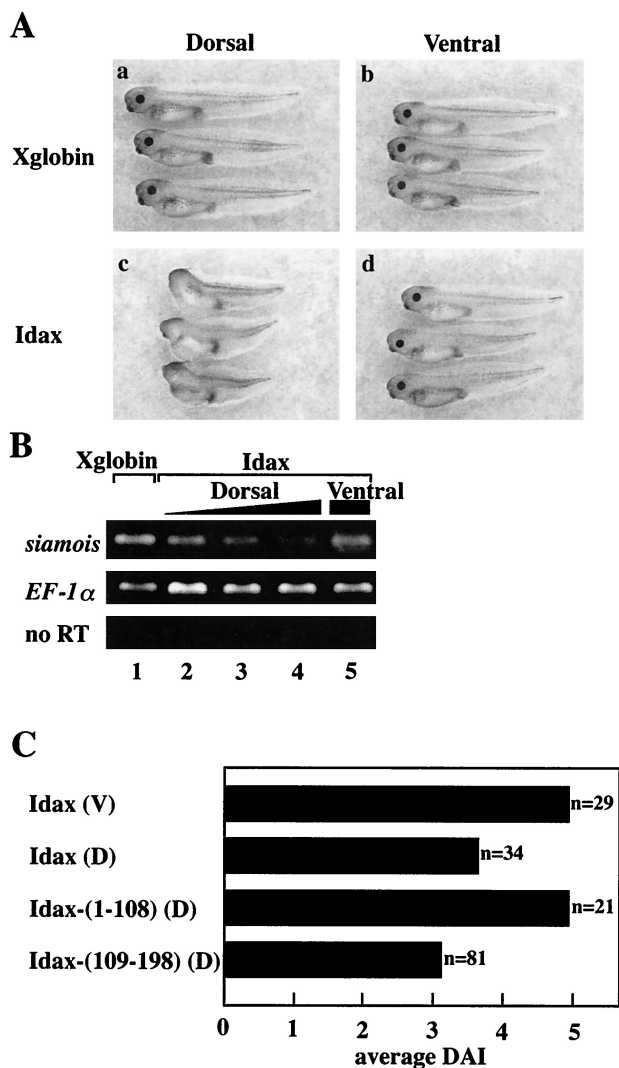


FIG. 6. Effects of Idax on axis formation in *Xenopus* embryos. (A) Ventralizing activity of Idax. (a) Dorsal injection of Xglobin (1 ng). (b) Ventral injection of Xglobin. (c) Dorsal injection of Idax (200 pg). (d) Ventral injection of Idax. (B) Inhibition of *siamois* expression by Idax. *siamois* expression in embryos was detected with RT-PCR analysis. Shown are dorsal injection with Xglobin (lane 1, 1 ng); dorsal injection with Idax (lane 2, 50 pg; lane 3, 100 pg; lane 4, 200 pg); and ventral injection with Idax (lane 5, 200 pg). The amounts of cDNA were standardized with *EF-1α*. no RT, experiments without RT-PCR. (C) Ventralizing activity of Idax deletion mutants. Embryos were injected ventrally (V) or dorsally (D) with Idax (full length) or dorsally with Idax-(1-108) or Idax-(109-198). The phenotypes were expressed as DAI. DAI 0, completely ventralized; DAI 5, normal.

formation during gastrulation and *Lef-1* is necessary for hair development at later stages in the mouse (39, 63, 67). Thus, components involved in the Wnt signaling pathway should be expressed during gastrulation or later. We have shown that Idax is expressed at these stages, from embryonic days 7 to 17, suggesting that this gene is likely to be involved in the Wnt signaling pathway at the appropriate time.

The PDZ domain is conserved in many proteins and generally acts as a protein-interacting module (8). The PDZ domain can form a dimer, and a unique amino acid motif, S/T-X-V in the C terminus, is known to bind to the PDZ domain (58). Idax

does not have this sequence in the C terminus, and the three C-terminal amino acids are not necessary for the binding of Idax to the PDZ domain of Dvl (data not shown). Although we have found that the C-terminal half of Idax is necessary for its interaction with Dvl, the minimal region of Idax required for binding to Dvl remains to be clarified. Several proteins have been reported to form a complex with the PDZ domain of Dvl. These are casein kinase Iε (CKIε) (47, 51), CKII (68), protein phosphatase 2C (PP2C) (59), and Frat (37). As none of these proteins contain the S/T-X-V sequence in their C termini, the PDZ domain of Dvl may have different properties from those of other known PDZ domains regarding protein-protein interactions.

CKIε and CKII associate with and phosphorylate Dvl (47, 51, 68). Expression of CKIε in *Xenopus* embryos induces β-catenin accumulation, *siamois* expression, and secondary axis formation, whereas GSK-3 blocks the ability of CKIε to rescue UV-induced axial deficiencies in *Xenopus* embryos (47). These results suggest that CKIε functions between Dvl and GSK-3 and that it regulates the Wnt signaling pathway positively. However, the molecular mechanism by which CKIε regulates the Wnt pathway is not known. Although the interaction with CKII requires the region containing the PDZ domain, whether this interaction is direct is not known and its significance in the Wnt signaling pathway is not yet clear. PP2C has been isolated by the yeast two-hybrid method using the PDZ domain as bait (59). Expression of PP2C in COS cells dephosphorylates and down-regulates Axin and stimulates the transcriptional activity of *Lef-1* (59). These results suggest that PP2C works as a positive regulator of the Wnt signaling pathway by inhibiting phosphorylation in the Axin complex. GBP (GSK-3-binding protein) was originally identified as a *Xenopus* GSK-3-binding protein that inhibits GSK-3 activity and mimics the effects of Wnt in *Xenopus* embryos, and Frat is a mammalian homolog of GBP (74). It has been suggested that the PDZ domain of Dvl binds to Frat and that Dvl recruits Frat to the Axin complex, thereby inducing the dissociation of GSK-3 from Axin in response to Wnt (37). Therefore, Frat also regulates the Wnt signaling pathway positively.

In contrast to the action of CKIε, PP2C, and Frat, Idax functions as a negative regulator of the Wnt signaling pathway. Several possible mechanisms for the mode of action of Idax are conceivable. The first is that Idax competes with CKIε, PP2C, or Frat for the interaction with Dvl, thereby suppressing their positive regulation of the Wnt pathway. The second possibility is that Idax relieves the repressive action of Dvl on Axin by inhibiting their interaction. However, the latter may be unlikely, because the affinity of Dvl for Idax is lower than that of Dvl for Axin. Nevertheless, one interesting possibility is that Wnt activates a protein kinase which phosphorylates Dvl or Idax, thereby modulating their affinities. Indeed, Dvl is phosphorylated in several cell lines treated with Wnt-3a (35). As CKIε or CKII phosphorylates Dvl in vitro, these protein kinases may modify the affinities of Dvl for Idax and Axin. The third possibility is that Idax may disrupt the tertiary conformation of Dvl by interacting with the PDZ domain of Dvl. It has been suggested that the tertiary conformation of the PDZ domain brings together the DIX and the DEP domains to form a functional unit (49). We have shown that the region containing the DIX domain of Dvl is important for its direct interac-

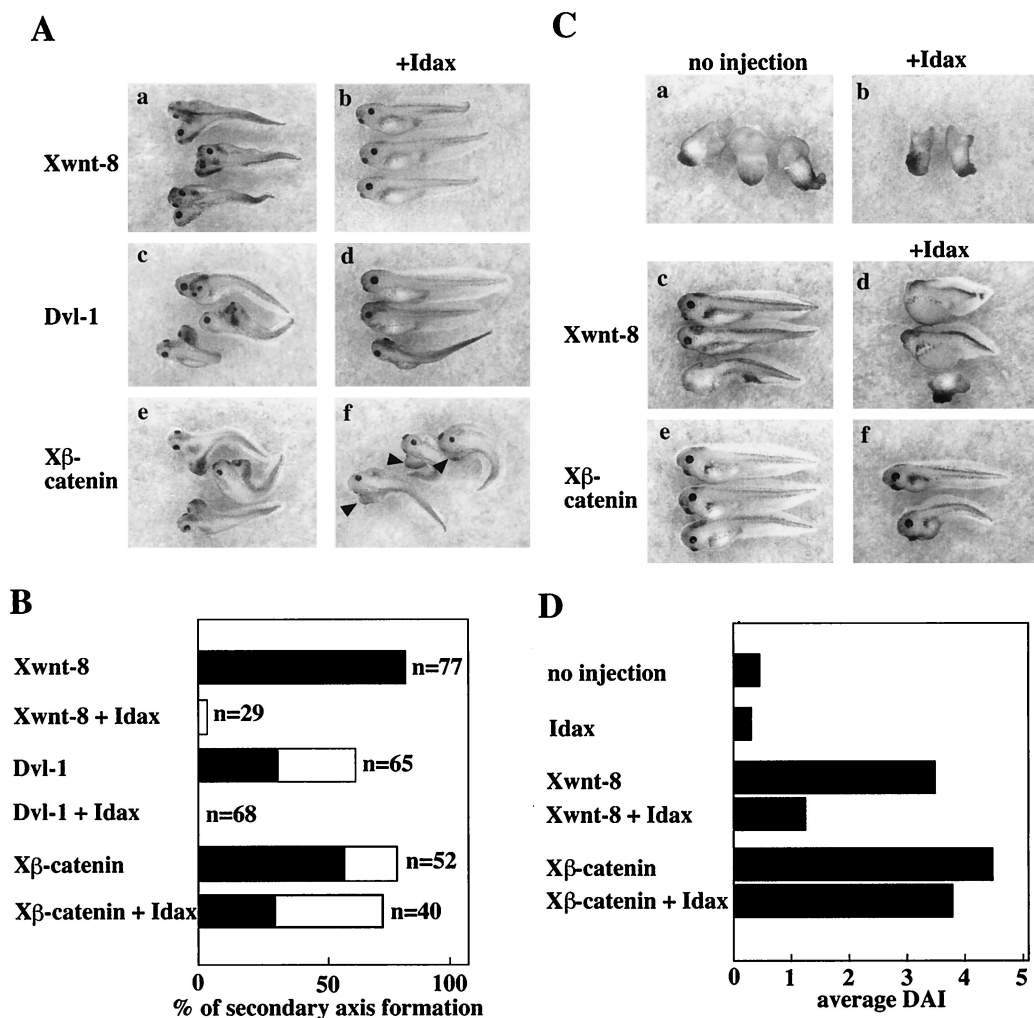


FIG. 7. Effects of Idax on Wnt signal-dependent axis formation. (A) Effects of Idax on Wnt signal-dependent secondary axis formation. Embryos were injected ventrally with Xwnt-8 (40 pg) (a), Xwnt-8 and Idax (200 pg) (b), Dvl-1 (1 ng) (c), Dvl-1 and Idax (d), Xβ-catenin (1 ng) (e), or Xβ-catenin and Idax (f). Arrowheads in panel f indicate secondary axes. (B) The results from panel A are expressed as percentage of secondary axis formation. Black bars show complete axis duplication, which includes eyes and cement glands. White bars indicate incomplete axis duplication characterized by a lack of head structures but with a distinct branched axis. (C) Effects of Idax on Wnt-dependent rescue of axis formation. UV-treated embryos were injected with nothing (a), Idax (200 pg) (b), Xwnt-8 (40 pg) (c), Xwnt-8 and Idax (d), Xβ-catenin (1 ng) (e), or Xβ-catenin and Idax (f). (D) The results from panel C are expressed as DAI.

tion with Axin and for Wnt signaling (27, 45). It is intriguing to speculate that the PDZ domain is necessary for maintaining the conformation of the DIX domain of Dvl to bind to Axin and that Idax causes a conformational change in Dvl, thereby preventing the binding of Dvl to Axin indirectly.

β-catenin is present in a complex including Axin, GSK-3β, APC, Dvl, and Frat, where its stability is regulated. Inhibition of GSK-3β or its dissociation from the complex by Dvl-Frat in response to Wnt could be critical for the disassembly of this complex. The results presented here may elucidate an additional part in the regulation of the Wnt signaling pathway. We have recently found Axam as an additional component in the Wnt signaling pathway (23). Axam is an Axin-binding protein that relieves the repression by Dvl of Axin's function, thereby leading to down-regulation of β-catenin. Although Axam inhibits complex formation between Dvl and Axin, how Idax affects the function of Axam is not known. The molecular

mechanism by which Wnt regulates the assembly and disassembly of this complicated complex remains to be clarified.

#### ACKNOWLEDGMENTS

We are grateful to H. Clevers, D. Kimelman, B. Dallapiccola, A. Nagafuchi, and M. Nakata for donating plasmids and antibodies. We thank the Research Center for Molecular Medicine and Research Facilities for Laboratory Animal Sciences, Hiroshima University School of Medicine, for the use of their facilities.

This work was supported by grants-in-aid for scientific research (B) and for scientific research on priority areas (A) from the Ministry of Education, Science, and Culture, Japan (1999 and 2000), by grants from the Yamanouchi Foundation for Research on Metabolic Disorders (1999 and 2000), by the Uehara Memorial Foundation (1998), by a Research Grant of the Princess Takamatsu Cancer Research Fund (1999; 99-23195), and by the Public Trust Haraguchi Memorial Cancer Research Fund (1999).

## REFERENCES

- Axelrod, J. D., J. R. Miller, J. M. Shulman, R. T. Moon, and N. Perrimon. 1998. Differential recruitment of Dishevelled provides signaling specificity in the planar cell polarity and Wingless signaling pathways. *Genes Dev.* **12**: 2610–2622.
- Behrens, J., B.-A. Jerchow, M. Würtele, J. Grimm, C. Asbrand, R. Wirtz, M. Kühl, D. Wedlich, and W. Birchmeier. 1998. Functional interaction of an Axin homolog, conductin, with  $\beta$ -catenin, APC, and GSK3 $\beta$ . *Science* **280**: 596–599.
- Behrens, J., J. P. von Kries, M. Kühl, L. Bruhn, D. Wedlich, R. Grosschedl, and W. Birchmeier. 1996. Functional interaction of  $\beta$ -catenin with the transcription factor LEF-1. *Nature* **382**:638–642.
- Boutros, M., N. Paricio, D. I. Strutt, and M. Mlodzik. 1998. Dishevelled activates JNK and discriminates between JNK pathways in planar polarity and wingless signaling. *Cell* **94**:109–118.
- Bradford, M. M. 1976. A rapid and sensitive method for the quantitation of microgram quantities of protein utilizing the principle of protein-dye binding. *Anal. Biochem.* **72**:248–254.
- Brannon, M., M. Gomperts, L. Sumoy, R. T. Moon, and D. Kimelman. 1997. A  $\beta$ -catenin/XTcf-3 complex binds to the *siamois* promoter to regulate dorsal axis specification in *Xenopus*. *Genes Dev.* **11**:2359–2370.
- Cadigan, K. M., and R. Nusse. 1997. Wnt signaling: a common theme in animal development. *Genes Dev.* **11**:3286–3305.
- Craven, S. E., and D. S. BREDD. 1998. PDZ proteins organize synaptic signaling pathways. *Cell* **93**:495–498.
- Dale, T. C. 1998. Signal transduction by the Wnt family of ligands. *Biochem. J.* **329**:209–223.
- Fagotto, F., E. Jho, L. Zeng, T. Kurth, T. Joos, C. Kaufmann, and F. Costantini. 1999. Domains of Axin involved in protein-protein interactions, Wnt pathway inhibition, and intracellular localization. *J. Cell Biol.* **145**:741–756.
- Funayama, N., F. Fagotto, P. McCrea, and B. M. Gumbiner. 1995. Embryonic axis induction by the armadillo repeat domain of  $\beta$ -catenin: evidence for intracellular signaling. *J. Cell Biol.* **128**:959–968.
- Hart, M., J.-P. Concordet, I. Lassot, I. Albert, R. del los Santos, H. Durand, C. Perret, B. Rubinfeld, F. Margottin, R. Benarous, and P. Polakis. 1999. The F-box protein  $\beta$ -TrCP associates with phosphorylated  $\beta$ -catenin and regulates its activity in the cell. *Curr. Biol.* **9**:207–210.
- Hart, M. J., R. de los Santos, I. N. Albert, B. Rubinfeld, and P. Polakis. 1998. Downregulation of  $\beta$ -catenin by human Axin and its association with the APC tumor suppressor,  $\beta$ -catenin and GSK-3 $\beta$ . *Curr. Biol.* **8**:573–581.
- He, T.-C., T. A. Chan, B. Vogelstein, and K. W. Kinzler. 1999. PPAR $\delta$  is an APC-regulated target of nonsteroidal anti-inflammatory drugs. *Cell* **99**:335–345.
- He, T.-C., A. B. Sparks, C. Rago, H. Hermeking, L. Zawel, L. T. da Costa, P. J. Morin, B. Vogelstein, and K. W. Kinzler. 1998. Identification of c-MYC as a target of the APC pathway. *Science* **281**:1509–1512.
- Heisenberg, C. P., M. Tada, G. J. Rauch, L. Saúde, M. L. Concha, R. Geisler, D. L. Stemple, J. C. Smith, and S. W. Wilson. 2000. Silberblick/Wnt11 mediates convergent extension movements during zebrafish gastrulation. *Nature* **405**:76–81.
- Huber, O., R. Korn, J. McLaughlin, M. Ohsugi, B. G. Herrmann, and R. Kemler. 1996. Nuclear localization of  $\beta$ -catenin by interaction with transcription factor LEF-1. *Mech. Dev.* **59**:3–10.
- Huelsken, J., R. Vogel, V. Brinkmann, B. Erdmann, C. Birchmeier, and W. Birchmeier. 2000. Requirement for  $\beta$ -catenin in anterior-posterior axis formation in mice. *J. Cell Biol.* **148**:567–578.
- Ikeda, S., M. Kishida, Y. Matsuura, H. Usui, and A. Kikuchi. 2000. GSK-3 $\beta$ -dependent phosphorylation of adenomatous polyposis coli gene product can be modulated by  $\beta$ -catenin and protein phosphatase 2A complexed with Axin. *Oncogene* **19**:537–545.
- Ikeda, S., S. Kishida, H. Yamamoto, H. Murai, S. Koyama, and A. Kikuchi. 1998. Axin, a negative regulator of the Wnt signaling pathway, forms a complex with GSK-3 $\beta$  and  $\beta$ -catenin and promotes GSK-3 $\beta$ -dependent phosphorylation of  $\beta$ -catenin. *EMBO J.* **17**:1371–1384.
- Itoh, K., A. Antipova, M. J. Ratcliffe, and S. Sokol. 2000. Interaction of Dishevelled and *Xenopus* Axin-related protein is required for Wnt signal transduction. *Mol. Cell Biol.* **20**:2228–2238.
- Itoh, K., V. E. Krupnik, and S. Y. Sokol. 1998. Axis determination in *Xenopus* involves biochemical interactions of axin, glycogen synthase kinase 3 and  $\beta$ -catenin. *Curr. Biol.* **8**:591–594.
- Kadaya, T., S. Kishida, A. Fukui, T. Hinoi, T. Michiue, M. Asashima, and A. Kikuchi. Inhibition of Wnt signaling pathway by a novel Axin-binding protein. *J. Biol. Chem.*, in press.
- Kao, K. R., and R. P. Elinson. 1988. The entire mesodermal mantle behaves as Spemann's organizer in dorsoanterior enhanced *Xenopus laevis* embryos. *Dev. Biol.* **127**:64–77.
- Kikuchi, A. 1999. Roles of Axin in the Wnt signalling pathway. *Cell. Signal.* **11**:777–788.
- Kishida, M., S. Koyama, S. Kishida, K. Matsubara, S. Nakashima, K. Higano, R. Takada, S. Takada, and A. Kikuchi. 1999. Axin prevents Wnt-3a-induced accumulation of  $\beta$ -catenin. *Oncogene* **18**:979–985.
- Kishida, S., H. Yamamoto, S.-I. Hino, S. Ikeda, M. Kishida, and A. Kikuchi. 1999. DIX domains of Dvl and Axin are necessary for protein interactions and their ability to regulate  $\beta$ -catenin stability. *Mol. Cell Biol.* **19**:4414–4422.
- Kishida, S., H. Yamamoto, S. Ikeda, M. Kishida, I. Sakamoto, S. Koyama, and A. Kikuchi. 1998. Axin, a negative regulator of the Wnt signaling pathway, directly interacts with adenomatous polyposis coli and regulates the stabilization of  $\beta$ -catenin. *J. Biol. Chem.* **273**:10823–10826.
- Kitagawa, M., S. Hatakeyama, M. Shirane, M. Matsumoto, N. Ishida, K. Hattori, I. Nakamichi, A. Kikuchi, K.-I. Nakayama, and K. Nakayama. 1999. An F-box protein, FWD1, mediates ubiquitin-dependent proteolysis of  $\beta$ -catenin. *EMBO J.* **18**:2401–2410.
- Klingensmith, J., R. Nusse, and N. Perrimon. 1994. The *Drosophila* segment polarity gene *dishevelled* encodes a novel protein required for response to the wingless signal. *Genes Dev.* **8**:118–130.
- Klingensmith, J., Y. Yang, J. D. Axelrod, D. R. Beier, N. Perrimon, and D. J. Sussman. 1996. Conservation of *dishevelled* structure and function between flies and mice: isolation and characterization of *Dvl2*. *Mech. Dev.* **58**:15–26.
- Korinek, V., N. Barker, P. J. Morin, D. van Wichen, R. de Weger, K. W. Kinzler, B. Vogelstein, and H. Clevers. 1997. Constitutive transcriptional activation by a  $\beta$ -catenin-Tcf complex in APC<sup>-/-</sup> colon carcinoma. *Science* **275**:1784–1787.
- Kozak, M. 1987. An analysis of 5'-noncoding sequences from 699 vertebrate messenger RNAs. *Nucleic Acids Res.* **15**:8125–8148.
- Kreig, P. A., and D. A. Melton. 1984. Functional messenger RNAs are produced by SP6 *in vitro* transcription of cloned cDNAs. *Nucleic Acids Res.* **12**:7057–7070.
- Lee, J.-S., A. Ishimoto, and S.-I. Yanagawa. 1999. Characterization of mouse dishevelled (Dvl) proteins in Wnt/Wingless signaling pathway. *J. Biol. Chem.* **274**:21464–21470.
- Lemaire, P., N. Garrett, and J. B. Gurdon. 1995. Expression cloning of *Siamois*, a *Xenopus* homeobox gene expressed in dorsal-vegetal cells of blastulae and able to induce a complete secondary axis. *Cell* **81**:85–94.
- Li, L., H. Yuan, C. D. Weaver, J. Mao, G. H. Farr III, D. J. Sussman, J. Jonkers, D. Kimelman, and D. Wu. 1999. Axin and Frat1 interact with Dvl and GSK, bridging Dvl to GSK in Wnt-mediated regulation of LEF-1. *EMBO J.* **18**:4233–4240.
- Li, L., H. Yuan, W. Xie, J. Mao, A. M. Caruso, A. McMahon, D. J. Sussman, and D. Wu. 1999. Dishevelled proteins lead to two signaling pathways. *J. Biol. Chem.* **274**:129–134.
- Liu, P., M. Wakamiya, M. J. Shea, U. Albrecht, R. R. Behringer, and A. Bradley. 1999. Requirement for *Wnt3* in vertebrate axis formation. *Nat. Genet.* **22**:361–365.
- Maniatis, T. 1982. Molecular cloning: a laboratory manual. Cold Spring Harbor Laboratory, Cold Spring Harbor, N.Y.
- Mann, B., M. Gelos, A. Siedow, M. L. Hanski, A. Gratchev, M. Ilyas, W. F. Bodmer, M. P. Moyer, E. O. Riecken, H. J. Buhr, and C. Hanski. 1999. Target genes of  $\beta$ -catenin-T cell-factor/lymphoid-enhancer-factor signaling in human colorectal carcinomas. *Proc. Natl. Acad. Sci. USA* **96**:1603–1608.
- Miller, J. R., A. M. Hocking, J. D. Brown, and R. T. Moon. 1999. Mechanism and function of signal transduction by the Wnt/ $\beta$ -catenin and Wnt/Ca<sup>2+</sup> pathways. *Oncogene* **18**:7860–7872.
- Molenaar, M., M. van de Wetering, M. Oosterwegel, J. Peterson-Maduro, S. Godsave, V. Korinek, J. Roose, O. Destree, and H. Clevers. 1996. XTcf-3 transcription factor mediates  $\beta$ -catenin-induced axis formation in *Xenopus* embryos. *Cell* **86**:391–399.
- Moon, R. T., and D. Kimelman. 1998. From cortical rotation to organizer gene expression: toward a molecular explanation of axis specification in *Xenopus*. *Bioessays* **20**:536–545.
- Moriguchi, T., K. Kawachi, S. Kamakura, N. Masuyama, H. Yamanaka, K. Matsumoto, A. Kikuchi, and E. Nishida. 1999. Distinct domains of mouse dishevelled are responsible for the c-Jun N-terminal kinase/stress-activated protein kinase activation and the axis formation in vertebrates. *J. Biol. Chem.* **274**:30957–30962.
- Nakashima, S., K. Morinaka, S. Koyama, M. Ikeda, M. Kishida, K. Okawa, A. Iwamatsu, S. Kishida, and A. Kikuchi. 1999. Small G protein Ral and its downstream molecules regulate endocytosis of EGF and insulin receptors. *EMBO J.* **18**:3629–3642.
- Peters, J. M., R. M. McKay, J. P. McKay, and J. M. Graff. 1999. Casein kinase I transduces Wnt signals. *Nature* **401**:345–350.
- Pizzuti, A., F. Amati, G. Calabrese, A. Mari, A. Colosimo, V. Silani, L. Giardino, A. Ratti, D. Penso, L. Calzà, G. Palka, G. Scarlato, G. Novelli, and B. Dallapiccola. 1996. cDNA characterization and chromosomal mapping of two human homologues of the *Drosophila dishevelled* polarity gene. *Hum. Mol. Genet.* **5**:953–958.
- Rothbacher, U., M. N. Laurent, M. A. Deardorff, P. S. Klein, K. W. Y. Cho, and S. E. Fraser. 2000. Dishevelled phosphorylation, subcellular localization and multimerization regulate its role in early embryogenesis. *EMBO J.* **19**:1010–1022.
- Sakamoto, I., S. Kishida, A. Fukui, M. Kishida, H. Yamamoto, S.-I. Hino, T. Michiue, S. Takada, M. Asashima, and A. Kikuchi. 2000. A novel  $\beta$ -catenin-binding protein inhibits  $\beta$ -catenin-dependent tcf activation and axis forma-

- tion. *J. Biol. Chem.* **275**:32871–32878.
51. Sakanaka, C., P. Leong, L. Xu, S. D. Harrison, and L. T. Williams. 1999. Casein kinase I $\epsilon$  in the wnt pathway: regulation of  $\beta$ -catenin function. *Proc. Natl. Acad. Sci. USA* **96**:12548–12552.
  52. Sakanaka, C., J. B. Weiss, and L. T. Williams. 1998. Bridging of  $\beta$ -catenin and glycogen synthase kinase-3 $\beta$  by Axin and inhibition of  $\beta$ -catenin-mediated transcription. *Proc. Natl. Acad. Sci. USA* **95**:3020–3023.
  53. Scharf, S. R., and J. C. Gerhart. 1980. Determination of the dorsal-ventral axis in eggs of *Xenopus laevis*: complete rescue of uv-impaired eggs by oblique orientation before first cleavage. *Dev. Biol.* **79**:181–198.
  54. Shibamoto, S., K. Higano, R. Takada, F. Ito, M. Takeichi, and S. Takada. 1998. Cytoskeletal reorganization by soluble Wnt-3a protein signalling. *Genes Cells* **3**:659–670.
  55. Shtutman, M., J. Zhurinsky, I. Simcha, C. Albanese, M. D'Amico, R. Pestell, and A. Ben-Ze'ev. 1999. The cyclin D1 gene is a target of the  $\beta$ -catenin/LEF-1 pathway. *Proc. Natl. Acad. Sci. USA* **96**:5522–5527.
  56. Smalley, M. J., E. Sara, H. Paterson, S. Naylor, D. Cook, H. Jayatilake, L. G. Fryer, L. Hutchinson, M. J. Fry, and T. C. Dale. 1999. Interaction of Axin and Dvl-2 proteins regulates Dvl-2 stimulated TCF-dependent transcription. *EMBO J.* **18**:2823–2835.
  57. Sokol, S. Y. 1996. Analysis of Dishevelled signalling pathways during *Xenopus* development. *Curr. Biol.* **6**:1456–1467.
  58. Songyang, Z., A. S. Fanning, C. Fu, J. Xu, S. M. Marfatia, A. H. Chishti, A. Crompton, A. C. Chan, J. M. Anderson, and L. C. Cantley. 1997. Recognition of unique carboxyl-terminal motifs by distinct PDZ domains. *Science* **275**:73–77.
  59. Strovel, E. T., D. Wu, and D. J. Sussman. 2000. Protein phosphatase 2C $\alpha$  dephosphorylates Axin and activates LEF-1-dependent transcription. *J. Biol. Chem.* **275**:2399–2403.
  60. Strutt, D. I., U. Weber, and M. Mlodzik. 1997. The role of RhoA in tissue polarity and Frizzled signalling. *Nature* **387**:292–295.
  61. Sussman, D. J., J. Klingensmith, P. Salinas, P. S. Adams, R. Nusse, and N. Perrimon. 1994. Isolation and characterization of a mouse homolog of the *Drosophila* segment polarity gene *dishevelled*. *Dev. Biol.* **166**:73–86.
  62. Tada, M., and J. C. Smith. 2000. Xwnt11 is a target of *Xenopus* Brachyury: regulation of gastrulation movements via Dishevelled, but not through the canonical Wnt pathway. *Development* **127**:2227–2238.
  63. Takada, S., K. L. Stark, M. J. Shea, G. Vassileva, J. A. McMahon, and A. P. McMahon. 1994. *Wnt-3a* regulates somite and tailbud formation in the mouse embryo. *Genes Dev.* **8**:174–189.
  64. Tetsu, O., and F. McCormick. 1999.  $\beta$ -Catenin regulates expression of cyclin D1 in colon carcinoma cells. *Nature* **398**:422–426.
  65. Theisen, H., J. Purcell, M. Bennett, D. Kansagara, A. Syed, and J. L. Marsh. 1994. *Dishevelled* is required during *wingless* signaling to establish both cell polarity and cell identity. *Development* **120**:347–360.
  66. Tian, Q., T. Nakayama, M. P. Dixon, and J. L. Christian. 1999. Post-transcriptional regulation of Xwnt-8 expression is required for normal myogenesis during vertebrate embryonic development. *Development* **126**:3371–3380.
  67. van Genderen, C., R. M. Okamura, I. Fariñas, R.-G. Quo, T. G. Parslow, L. Bruhn, and R. Grosschedl. 1994. Development of several organs that require inductive epithelial-mesenchymal interactions is impaired in *LEF-1*-deficient mice. *Genes Dev.* **8**:2691–2703.
  68. Willert, K., M. Brink, A. Wodarz, H. Varmus, and R. Nusse. 1997. Casein kinase 2 associates with phosphorylates Dishevelled. *EMBO J.* **16**:3089–3096.
  69. Wodarz, A., and R. Nusse. 1998. Mechanisms of Wnt signaling in development. *Annu. Rev. Cell Dev. Biol.* **14**:59–88.
  70. Yamamoto, H., S. Kishida, M. Kishida, S. Ikeda, S. Takada, and A. Kikuchi. 1999. Phosphorylation of Axin, a Wnt signal negative regulator, by glycogen synthase kinase-3 $\beta$  regulates its stability. *J. Biol. Chem.* **274**:10681–10684.
  71. Yamamoto, H., S. Kishida, T. Uochi, S. Ikeda, S. Koyama, M. Asashima, and A. Kikuchi. 1998. Axin, a member of the Axin family, interacts with both glycogen synthase kinase 3 $\beta$  and  $\beta$ -catenin and inhibits axis formation of *Xenopus* embryos. *Mol. Cell. Biol.* **18**:2867–2875.
  72. Yanagawa, S.-I., J.-S. Lee, T. Haruna, H. Oda, T. Uemura, M. Takeichi, and A. Ishimoto. 1997. Accumulation of Armadillo induced by Wingless, Dishevelled, and dominant-negative Zeste-white 3 leads to elevated DE-cadherin in *Drosophila* clone 8 wing disc cells. *J. Biol. Chem.* **272**:25243–25251.
  73. Yanagawa, S.-I., F. van Leeuwen, A. Wodarz, J. Klingensmith, and R. Nusse. 1995. The Dishevelled protein is modified by Wingless signaling in *Drosophila*. *Genes Dev.* **9**:1087–1097.
  74. Yost, C., G. H. Farr III, S. B. Pierce, D. M. Ferkey, M. M. Chen, and D. Kimelman. 1998. GBP, an inhibitor of GSK-3, is implicated in *Xenopus* development and oncogenesis. *Cell* **93**:1031–1041.
  75. Yost, C., M. Torres, J. R. Miller, E. Huang, D. Kimelman, and R. T. Moon. 1996. The axis-inducing activity, stability, and subcellular distribution of  $\beta$ -catenin is regulated in *Xenopus* embryos by glycogen synthase kinase 3. *Genes Dev.* **10**:1443–1454.
  76. Zeng, L., F. Fagotto, T. Zhang, W. Hsu, T. J. Vasicsek, W. L. Perry III, J. J. Lee, S. M. Tilghman, B. M. Gumbiner, and F. Costantini. 1997. The mouse *Fused* locus encodes Axin, an inhibitor of the Wnt signaling pathway that regulates embryonic axis formation. *Cell* **90**:181–192.